Id2-Mediated Inhibition of E2A Represses Memory CD8$^+$ T Cell Differentiation

Frederick Masson,* Martina Minnich,† Moshe Olshansky,‡ Ivan Bilic,†,[1] Adele M. Mount,†,[2] Axel Kallies,*,§ Terence P. Speed,‡,¶ Meinrad Busslinger,† Stephen L. Nutt,*,§ and Gabrielle T. Belz*,§

The transcription factor inhibitor of DNA binding (Id)2 modulates T cell fate decisions, but the molecular mechanism underpinning this regulation is unclear. In this study we show that loss of Id2 cripples effector differentiation and instead programs CD8$^+$ T cells to adopt a memory fate with increased *Eomesodermin* and *Tcf7* expression. We demonstrate that Id2 restrains CD8$^+$ T cell memory differentiation by inhibiting E2A-mediated direct activation of *Tcf7* and that Id2 expression level mirrors T cell memory recall capacity. As a result of the defective effector differentiation, Id2-deficient CD8$^+$ T cells fail to induce sufficient *Tbx21* expression to generate short-lived effector CD8$^+$ T cells. Our findings reveal that the Id2/E2A axis orchestrates T cell differentiation through the induction or repression of downstream transcription factors essential for effector and memory T cell differentiation. ***The Journal of Immunology*****, 2013, 190: 4585–4594.**

Successful eradication and protection from reinfection by intracellular pathogens such as viruses and bacteria depend on the generation of effector and memory CD8$^+$ T cells. Naive CD8$^+$ T cells, on encounter with dendritic cells presenting pathogen Ags, undergo multiple rounds of proliferation and rapidly differentiate into short-lived Ag-specific effector T cells with cytotoxic and cytokine producing capacity. After resolution of the infection, effector CD8$^+$ T cell numbers contract significantly, leaving a small (5–10%) residual population of long-lived memory CD8$^+$ T cells poised to rapidly respond to a second encounter with the pathogen.

Several transcription factors are essential for the specification and differentiation of peripheral T cells following Ag encounter. These include the basic helix-loop-helix proteins inhibitor of DNA binding (Id)2 and Id3 (1–3), the T-box transcription factors T-bet and eomesodermin (Eomes) (4), B lymphocyte–induced maturation protein 1 (Blimp1) (5–7), Bcl-6 (8), and Tcf7 (also known as TCF-1) (9). T-bet (encoded by *Tbx21*) and Blimp1 (encoded by *Prdm1*) direct the terminal differentiation of effector T cells. Ablation of either T-bet or Blimp1 results in a complete loss of KLRG1$^+$IL-7R^{low} short-lived effector cells. Furthermore, T-bet drives effector cell formation in a dose-dependent manner at the expense of the formation of memory cells (10). Maintenance of memory cells appears to depend on the induction of *Eomes* (4). Although our understanding of *Eomes* regulation is incomplete, recent evidence suggests that Tcf7, a critical mediator of the Wnt/β-catenin pathway, regulates CD8$^+$ T cell memory by direct binding to the *Eomes* locus (9). However, the interactions among these transcription factors, as well as the signals that drive effector and memory CD8$^+$ T cell fate decisions, are still poorly understood.

It is now established that peripheral T cell differentiation is regulated by the activity of Id proteins (11). Four Id proteins (Id1, Id2, Id3, Id4), which lack a DNA-binding domain, are capable of binding the E proteins, E2A (possessing two isoforms, E47 and E12), HEB, and E2-2. The recent development of reporter mice for Id2 and Id3 has identified that these two transcriptional regulators are expressed in a reciprocal manner and regulate distinct functions in the differentiation of peripheral T cells (3). For example, Id2 is upregulated in effector T cells. In contrast, induction of Id3 reflects the emergence of precursors of long-lived memory T cells, and repression by Blimp1 limits formation of memory CD8$^+$ T cells, thus dispelling the notion that Id2 and Id3 are simply redundant (2, 3).

Id2 has multiple essential functions in the hematopoietic system. It is required for the development of CD103$^+$ and CD8α$^+$ dendritic cells, NK cells, a subset of intraepithelial T cells, and lymphoid tissue inducer cells (12, 13). In Ag-specific CD8$^+$ T cells, Id2 has been proposed to act mainly by regulating their survival during

*Division of Molecular Immunology, Walter and Eliza Hall Institute of Medical Research, Melbourne, Victoria 3052, Australia; †Research Institute of Molecular Pathology, Vienna Biocenter, 1030 Vienna, Austria; ‡Division of Bioinformatics, Walter and Eliza Hall Institute of Medical Research, Melbourne, Victoria 3052, Australia; §Department of Medical Biology, University of Melbourne, Melbourne, Victoria 3010, Australia; and ¶Department of Mathematics and Statistics, University of Melbourne, Melbourne, Victoria 3010, Australia

[1]Current address: Akron Molecules GmbH, Vienna, Austria.

[2]Current address: CSL Limited, Parkville, VIC, Australia.

Received for publication January 11, 2013. Accepted for publication February 20, 2013.

This work was supported by grants and fellowships from the National Health and Medical Research Council of Australia (to G.T.B., S.L.N., and T.P.S.), the Wellcome Trust (to G.T.B.), the Viertel Foundation and the Howard Hughes Medical Institute (to G.T.B.), the Australian Research Council (to T.P.S.), and the Australian Research Council Future Fellowship (to G.T.B., A.K., and S.L.N.). Research of the Busslinger Group was supported by Boehringer Ingelheim and the Genome Research in Austria initiative (financed by the Bundesminsterium für Bildung und Wissenschaft). This work was also supported by Victorian State Government operational infrastructure support and by the Australian Government National Health and Medical Research Council Independent Research Institute Infrastructure Support Scheme.

Address correspondence and reprint requests to Dr. Gabrielle T. Belz, Division of Molecular Immunology, Walter and Eliza Hall Institute of Medical Research, 1G Royal Parade, Parkville, VIC 3052, Australia. E-mail address: belz@wehi.edu.au

The online version of this article contains supplemental material.

Abbreviations used in this article: Blimp1, B lymphocyte–induced maturation protein 1; ChIP, chromatin immunoprecipitation; DE, differentially expressed; Eomes, eomesodermin; Gzm, granzyme; Id, inhibitor of DNA binding; i.n., intranasal(ly); IRES, internal ribosome entry site; Lm-OVA, *Listeria monocytogenes* encoding OVA; LN, lymph node; MSCV, murine stem cell virus; NP, nucleoprotein; PA, acidic polymerase; shRNA, short hairpin RNA.

infection (1), but the precise molecular mechanisms downstream of Id2 that determine T cell fate are poorly defined.

To understand this pathway in greater depth we generated mice with a reporter allele encoding GFP under the endogenous Id2 promoter (12) and a conditional allele allowing specific deletion of Id2 in T cells. This enabled us to examine the cellular and molecular pathway resulting from the loss of Id2 and to explore the mechanisms affecting effector and memory T cell fate outcomes in an infection setting. We demonstrated that Id2 was essential for the induction of high levels of *Tbx21* and this was required for the generation of short-lived effector $CD8^+$ cells. Loss of Id2 in $CD8^+$ T cells impaired effector T cell differentiation and programmed T cells to adopt a memory cell phenotype with increased *Eomes* and *Tcf7* expression. We also show that induction of Id2 restrains $CD8^+$ T cell memory differentiation by inhibiting E2A-mediated transactivation of *Tcf7* expression and that graded expression of Id2 rather than central or effector memory phenotype correlates with $CD8^+$ T cell memory recall capacity. Overall, we reveal that Id2 is a dose-dependent regulator of T cell differentiation by orchestrating the induction or repression of downstream transcription factors critical in effector versus memory differentiation.

Materials and Methods

Mice

$Id2^{gfp/gfp}$ (12), $Id2^{fl/fl}Lck^{Cre}$ ($Id2^{Lck}$), $Tbx21^{-/-}$ (14), OT-I (15), Flpe (16), LckCre (17), C57BL/6 ($Ly5.2^+$), B6.SJL-$Ptprc^a$ $Pepc^b$/BoyJ (B6.Ly5.1, $Ly5.1^+$), $Rosa26^{BirA/BirA}$ (18), and Ly5.1 × Ly5.2 (F_1) mice were used at 6–8 wk. $Id2^{fl/fl}$ mice were generated as described (19). All mice were bred and maintained under specific pathogen-free conditions in accordance with the guidelines of the Walter and Eliza Hall Institute of Medical Research Animal Ethics Committee.

Bacterial and viral infections

Mice were anesthetized with methoxyflurane and then inoculated with 10^4 PFU HKx31 (H3N2) influenza virus. Memory mice were generated by priming with i.p. injection of 10^7 PFU A/PR/8/34 (PR8) influenza virus (20). At the indicated times, mice were sacrificed, spleens, lymph nodes (LNs; mediastinal and superficial cervical), and lungs were removed, and single-cell suspension prepared for analysis. For listeria infection, recombinant *Listeria monocytogenes* encoding OVA (Lm-OVA) was grown in brain-heart infusion broth. Bacterial culture samples were grown to mid-log phase measured by OD (absorbance at 600 nm) and diluted in PBS for injection. Mice were infected i.v. with 2.5×10^3 rLm-OVA. Injected bacteria numbers were determined by spreading bacterial samples on brain-heart infusion plates followed by incubation overnight at 37°C.

Isolation of $CD8^+$ T cells

$CD8^+$ T cells were enriched from spleen and LNs by generating a single-cell suspension and incubating the cells in a mixture of optimally titrated Abs against Mac-1 (M1/70), Mac-3 (F4/80), Ter-119, GR1 (RB6-8C5), MHC class II (M5/114), and CD4 (GK1.5) for 30 min on ice. The Ab-bound cells were removed using anti-rat IgG Ab-conjugated magnetic beads (Dynabeads; Dynal).

Mononuclear cells were purified from the lung by generating single-cell suspensions, followed by centrifugation on Histopaque density gradient (1.077 g/ml; Sigma-Aldrich) for 18 min at 2000 rpm at room temperature. Liver-infiltrating lymphocytes were isolated by centrifugation liver cell suspension on an 80/40% Percoll (GE Healthcare Biosciences) density gradient for 20 min at 2500 rpm at room temperature.

Cell surface staining and FACS analysis

Virus-specific $CD8^+$ T cells were detected by staining with PE-coupled tetrameric H-2^b MHC class I complexes loaded with epitopes of influenza virus nucleoprotein (NP; $D^bNP_{366–374}$, H-$2D^b$–restricted) or acidic polymerase (PA; $D^bPA_{224–233}$, H-$2D^b$–restricted) as previously described (20). To block nonspecific binding of Abs, cells were incubated in rat IgG (1 mg/ml) together with anti–FcγR mAb (CD16/32, clone 2-4G21) for 10 min on ice. Samples were then stained with fluorochrome-labeled Abs against CD8α (53-6.7), CD62L (Mel-14), KLRG1 (2FY), IL-7R (A7R34), Ly5.1 (A20-1.1), Ly5.2 (104), and CD44 (IM7) (all from eBioscience or BD Pharmingen). Viable cells were analyzed by flow cytometry using propidium iodide or Sytox blue exclusion (Invitrogen). Analysis was performed on a FACSCanto or a FACS LSRFortessa (BD Biosciences) and data were analyzed using FlowJo flow cytometry analysis software.

Generation of bone marrow chimeras

Mixed bone marrow chimeras were established by reconstituting lethally irradiated (2 × 0.55 Gy) B6.Ly5.1 or Ly5.1 × Ly5.2 (F_1) recipient mice with a mixture of $Id2^{fl/fl}Lck^{Cre}$ (3.4×10^6) and wild-type ($Ly5.1^+$, 1.6×10^6) T cell–depleted bone marrow cells and allowed to reconstitute for 6–8 wk (5, 21).

Microarray analysis

$D^bNP_{366}{}^+CD8^+$ T cells were purified by flow cytometric sorting (FACSAria flow cytometer; BD Biosciences) from day 9 HKx31-infected PR8-primed $Id2^{gfp/gfp}$ or $Id2^{fl/fl}Lck^{Cre+}/Ly5.1^{+/+}$ mixed bone marrow chimeras. Total RNA was prepared using a Qiagen RNeasy Mini Kit (Qiagen) according to the manufacturer's instructions. DNA microarray analysis of gene expression was performed using Illumina MouseWG-6 v2.0 Expression BeadChip together with the manufacturer's probe annotation (released in November 2008). The Gene Expression Omnibus referenced accession nos. for these data are GSE44140 (http://www.ncbi.nlm.nih.gov/geo/query/acc.cgi?acc=GSE44140) and GSE44141 (http://www.ncbi.nlm.nih.gov/geo/query/acc.cgi?acc=GSE44141).

In vitro T cell culture analysis

$CD8^+$ T cells were enriched from the spleen of $Id2^{fl/fl}Lck^{Cre+}$ or wild-type mice. $CD8\alpha^+CD19^-$ T cells were purified either by FACS sorting or by two rounds of negative selection (MACS; Miltenyi Biotec) to obtain purities >95%. $CD8^+$ T cells were then cultured for 3 d in complete RPMI 1640 medium at 5×10^5 cells/well in plates coated with anti-CD3 mAb (5 μg/ml) together with anti-CD28 mAb (2 μg/ml) and recombinant human IL-2 (100 U/ml). Cells were then washed once and cultured (5×10^4 cells/ml) for 2 d, then replated at 6.7×10^4 cells/ml and cultured for an additional 2 d.

Retroviral constructs

Murine stem cell virus (MSCV)–T-bet–internal ribosome entry site (IRES)–GFP (10) has been previously described and MSCV-Id2-IRES-GFP and MSCV-IRES-GFP were a gift from Dr. Manabu Sugai (Kyoto University Hospital). *Tcfe2a*-IRES-GFP and IRES-GFP LMP vectors were a gift from Dr. Ross Dickins (Walter and Eliza Hall Institute).

Intracellular flow cytometry staining

For detection of intracellular granzyme (Gzm) B, T-bet and Eomes staining was performed directly ex vivo. GzmB was detected using anti-human GzmB Ab (GB12; Invitrogen) using a Cytofix/Cytoperm kit (BD Biosciences). Staining for T-bet (4B10; Santa Cruz Biotechnology) and Eomes (Dan11mag; eBioscience) used the Foxp3 kit (eBioscience).

Chromatin immunoprecipitation-PCR analysis

Chromatin immunoprecipitation (ChIP) was performed with an affinity-purified polyclonal rabbit Ab directed against the N-terminal peptide PRRRAANGGLDTQPKKVRKV of the mouse E2A protein. The precipitated DNA was quantified by real-time PCR analysis with SYBR Green, which was carried out on a MyiQ instrument (Bio-Rad). Primers sequences are supplied in Supplemental Table I.

Bio-ChIP sequencing

Total thymocytes (~10^8) from $Tcfe2a^{Bio/Bio}$ $Rosa26^{BirA/BirA}$ mice were used for chromatin precipitation by streptavidin pulldown (Bio-ChIP), as recently described in detail (22).

Quantitative RT-PCR

Total RNA was prepared from purified D^bNP_{366}-specific $CD8^+$ T cell populations using an RNeasy Mini Kit (Qiagen). cDNA was synthesized from total RNA with oligo(dT) and thermoscript reverse transcriptase (Invitrogen). Real-time PCR was performed using the SensiMix SYBR No-ROX Kit (Bioline). Analyses were done in triplicate and mean normalized expression was calculated with *Hprt* as the reference gene.

Retroviral transduction of OT-I TCR transgenic T cells

$Id2^{fl/fl}Lck^{Cre+}$ or wild-type $CD8^+$ OT-I T cells were enriched from the spleen and cultured in complete RPMI 1640 containing human recombi-

nant human IL-2 (30 U/ml) and 1 μg/ml $OVA_{257–264}$ peptide for 2 d. Retroviral supernatants were then spun for 1 h at 4000 rpm at 4°C in 12-well plates coated with 32 μg/ml RetroNectin. Retrovirus supernatant was then carefully removed from the plate and OT-I T cells were then added and cultured with human rIL-2 (30 U/ml) and polybrene (1 μg/ml) in complete RPMI 1640 for 1 d. For adoptive transfer experiments, OT-I T cells transduced with MSCV-T-bet-IRES-GFP, MSCV-Id2-IRES-GFP, or MSCV-IRES-GFP retroviruses were washed and expanded in a 75-cm^2 culture flask in the presence of IL-15 (20 ng/ml) for 4 d. GFP^+ cells were purified by flow cytometric sorting prior to adoptive transfer into recipient mice that were then infected the following day with Lm-OVA. OT-I cells transduced with the short hairpin RNA (shRNA) *Tcfe2a*-IRES-GFP LMP or IRES-GFP LMP retroviruses were selected in puromycin at 2 μg/ml for 5–7 d. Live cells were then purified by centrifugation on Histopaque density gradient before quantitative RT-PCR analysis.

Statistical analysis

Statistical analyses were performed using Prism software.

Results

Loss of Id2 impairs the differentiation of short-lived effector $CD8^+$ T cells

To map the expression level and the role of Id2 in different T cell populations, we made use of our previously described reporter allele where an IRES-GFP cassette has been inserted into the 3′ untranslated region of the Id2 gene by homologous recombination (12). To track the induction of Id2, wild-type and Id2 reporter mice ($Id2^{gfp/gfp}$) were infected intranasally (i.n.) with influenza A HKx31. Strikingly, Id2-GFP was rapidly upregulated in all influenza-specific D^bNP_{366}- and D^bPA_{224}-specific $CD8^+$ T cells regardless of their phenotype or anatomical location (Fig. 1A, 1B)

To examine how Id2 expression affected the emergence of influenza-specific $CD8^+$ effector and memory T cells, we analyzed mice that specifically lacked Id2 in T cells through LckCre-mediated deletion of the entire *Id2* coding region (19). To ex-

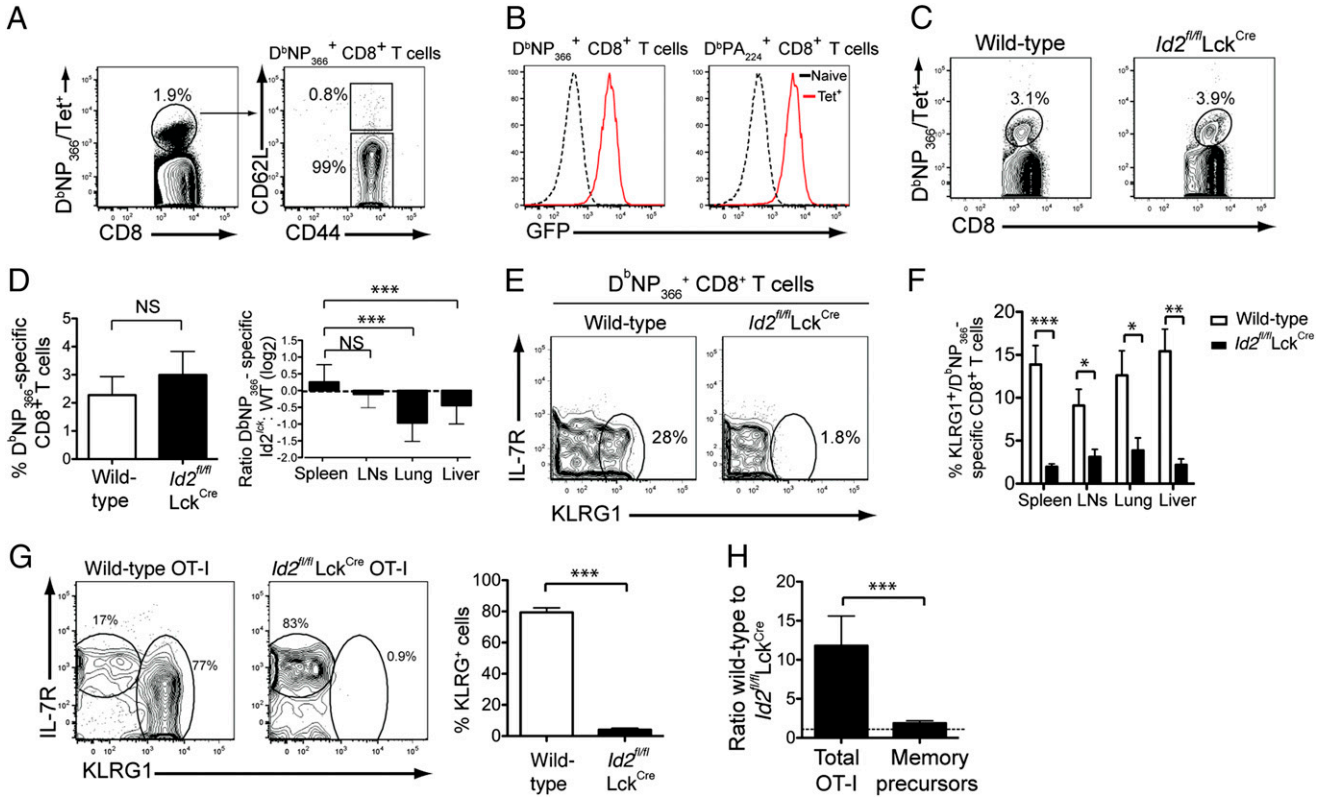

FIGURE 1. Id2-deficient $CD8^+$ T cells do not differentiate into $KLRG1^+$ effector cells. (**A**) $Id2^{gfp/gfp}$ and wild-type (+/+) mice were infected i.n. with influenza virus HKx31 and analyzed on day 9. (**B**) Id2-GFP expression in naive ($CD44^-CD62L^+$) and $D^bNP_{366}^+$ and $D^bPA_{224}^+$ influenza-specific $CD8^+$ T cells from spleen of infected mice. (**C**) Generation of wild-type and Id2-deficient D^bNP_{366}-specific $CD8^+$ T cells in $Ly5.2^+Id2Lck^{Cre+}$:$Ly5.1^+$ mixed bone marrow chimeric mice 10 d after i.n. influenza infection. Data are representative of 11 mice. (**D**) Frequency of D^bNP_{366}-specific $CD8^+$ T cells within the $Id2^{fl/fl}Lck^{Cre+}$ ($Ly5.2^+$) or the wild-type ($Ly5.1^+$) splenic $CD8^+$ T cell compartment from chimeric mice 10 d after HKx31 infection (*left panel*). Data are the means ± SEM from three independent experiments ($n = 11$). *Right panel*, Relative contribution of Id2-deficient $CD8^+$ T cells to the D^bNP_{366}-$CD8^+$ T cell populations in the indicated tissues (LNs, pooled superficial cervical and mediastinal LNs) expressed as $\log_2$ ratio of $D^bNP_{366}^+CD8^+$ T cells in $Id2^{fl/fl}Lck^{Cre+}$ and wild-type compartments. Data were normalized for the proportion of each genotype in the total $CD8^+$ T cells from the spleen and are pooled from two independent experiments ($n = 8$). (**E**) Bone marrow chimeric mice were infected with HKx31 and $D^bNP_{366}^+$ influenza-specific $CD8^+$ T cells in spleen were analyzed for the indicated markers within the wild-type ($Ly5.2^-$) and Id2-deficient ($Id2^{fl/fl}Lck^{Cre+}$, $Ly5.2^+$) compartments. Data are representative of at least three independent experiments. (**F**) Frequency of $KLRG1^+$ D^bNP_{366} $CD8^+$ T cells following primary HKx31 influenza infection. Data show the means ± SEM of $KLRG1^+$ influenza virus-specific cells within the $CD8^+$ T cell compartment in indicated tissues. For (E) and (F), data are pooled from three independent experiments ($n = 8$). (**G** and **H**) OT-I $Id2^{fl/fl}Lck^{Cre+}$ ($Ly5.2$) and OT-I wild-type ($Ly5.1 \times Ly5.2$) $CD8^+$ T cells, mixed in a 1:1 ratio, were transferred into wild-type $Ly5.1^+$ mice that were infected i.v. with Lm-OVA 24 h later. (G) Flow cytometric analysis of wild-type ($Ly5.1^+Ly5.2^+$ F1) or $Id2^{fl/fl}Lck^{Cre+}$ ($Ly5.2^+$) OT-I $CD8^+$ T cell population isolated from the spleen 9 d after infection with Lm-OVA. *Right panel*, Bar graph shows the mean percentage ± SEM of $KLRG1^+$ wild-type or $Id2^{fl/fl}Lck^{Cre+}$ OT-I $CD8^+$ T cell populations in the spleen. (H) Bar graph shows the mean ± SEM of the ratio of wild-type OT-I to $Id2^{fl/fl}Lck^{Cre+}$ OT-I T cells in total OT-I cells and in memory precursors cells ($IL\text{-}7R^{high}KLRG1^-$). Data are pooled from two independent experiments ($n = 10$). Statistically significant differences were determined using a two-tailed paired Student *t* test (A–G) or a Mann–Whitney nonparametric test (H). $*p < 0.05$, $**p < 0.01$, $***p < 0.001$.

clude secondary effects due to differing resolution of the infection in intact mice, Ly5.2$^+$*Id2*^{Lck} (fl/fl; Lck^{Cre+}) and Ly5.1$^+$Id2 (+/+) mixed bone marrow chimeras were generated and infected with influenza virus (HKx31). This revealed that the proportions of virus-specific CD8$^+$ T cells in Id2^{Lck} and wild-type compartments were similar in spleen and LNs (Fig. 1C, 1D). However, within the lung and liver, the relative frequency of *Id2*^{Lck} D^{b}NP$_{366}$- and D^{b}PA$_{224}$-specific CD8$^+$ T cells was reduced, suggesting a defect in the ability to migrate to and/or survive in nonlymphoid tissues (Fig. 1D). KLRG1$^+$IL-7R$^-$ short-lived effectors were selectively absent from the Id2-deficient CD8$^+$ T cell compartment in accordance with earlier observations (Fig. 1E, 1F, Supplemental Fig. 1) (3). The unaltered frequency of influenza-specific CD8$^+$ T cells in Id2-deficient and wild-type compartments within the spleen and LNs was surprising given a previous report that suggested Id2 was critical to control effector CD8$^+$ T cell survival (1). In this earlier study, Id2-deficient OVA-specific TCR transgenic CD8$^+$ T cells (OT-I) responding to systemic infection with rLm-OVA were highly susceptible to apoptosis mediated by the proapoptotic molecule Bim. To better understand the factors that underpin the discrepancies between the two studies, we analyzed the quantity and the quality of the response of *Id2*^{Lck} (Ly5.2$^+$) and wild-type (Ly5.1$^+$Ly5.2$^+$ F$_1$) OT-I T cells transferred into Ly5.1$^+$ recipients following i.v. Lm-OVA infection. Similar to previous results, *Id2*^{Lck} OT-I T cells were outcompeted by wild-type OT-I T cells at 9 d after Lm-OVA infection (Fig. 1G, 1H) (1). However, closer analysis revealed that following Lm-OVA infection most (~80%) wild-type OT-I T cells formed short-lived effectors whereas memory precursors represented a smaller proportion of the overall population. This short-lived effector population was absent in the *Id2*^{Lck} OT-I CD8$^+$ T cell compartment (Fig. 1G), but notably the memory precursor compartment was not affected by Id2 deficiency (Fig. 1H). This demonstrated that in the absence of Id2, the strong inflammatory stimulus of Lm-OVA resulted in the selective failure of the short-lived effector (IL-7R^{low}KLRG1$^+$) CD8$^+$ T cell subset to differentiate and/or survive. In contrast, memory precursor (IL-7R^{high}KLRG1$^-$) CD8$^+$ T cells were unaffected showing that Id2 loss does not globally impair virus-specific CD8$^+$ T cell survival.

Id2 expression restricts memory recall capacity

Id2 deficiency significantly affected effector T cell differentiation, but it was not clear whether normal memory was formed when Id2 was lacking. To understand the effect of Id2 loss on memory, we quantitated the proportion of influenza-specific memory CD8$^+$ T cells within the wild-type and Id2^{Lck} CD8$^+$ T cell compartments of mixed BM chimeras infected 9 wk previously with HKx31 virus (Fig. 2A, 2B). Neither the frequency of virus-specific memory CD8$^+$ T cells (Fig. 2A, 2B) nor the proportion of central memory T cells (F. Masson and G.T. Belz, unpublished observations) was significantly different from control cells. To accurately assess the recall potential of Id2-deficient memory T cells, CD8$^+$ T cells were enriched from the spleens of HKx31-infected mixed chimeric mice and adoptively transferred into naive recipients prior to influenza infection (Fig. 2C). Surprisingly, 10 d after infection, we found that Id2-deficient CD8$^+$ T cells had significantly increased in proportion compared with wild-type cells (Fig. 2D), indicating that Id2 expression restricts memory recall potential of CD8$^+$ T cells.

To understand the role of Id2 in the memory T cell compartment in more detail, we assessed the expression of Id2-GFP in Ag-specific CD8$^+$ T cells during the memory phase of influenza virus infection. Both effector memory and central memory T cells expressed a lower level of Id2-GFP than did acutely activated effector cells (Fig. 3A). Remarkably, approximately half of the

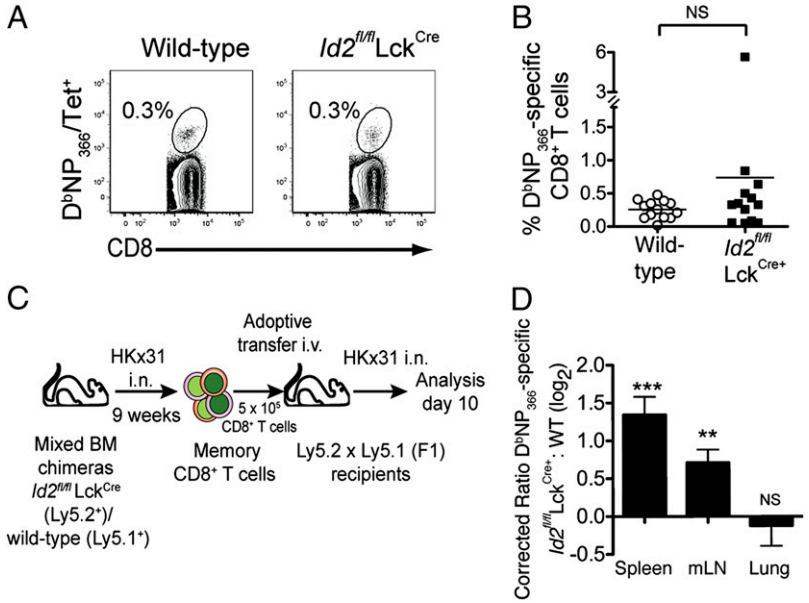

FIGURE 2. Id2-deficient memory CD8$^+$ T cells exhibit increased recall capacity. (**A** and **B**) Mixed bone marrow chimeras reconstituted with *Id2*$^{fl/fl}$Lck^{Cre+} (Ly5.2$^+$) and wild-type (Ly5.1$^+$) bone marrow were analyzed 9 wk after i.n. HKx31 infection. (A) Representative flow cytometric profiles and (B) cumulative analysis of the persistence of D^{b}NP$_{366}$-specific CD8$^+$ T cells within the *Id2*$^{fl/fl}$Lck^{Cre+} (Ly5.2$^+$) and the wild-type (Ly5.1$^+$) CD8$^+$ T cell compartments. Individual mice in (B) are shown by an open circle (wild-type) or filled square (*Id2*$^{fl/fl}$Lck^{Cre+}). Data are pooled from three independent experiments (n = 13). Statistically significant differences were determined using a paired two-tailed Student t test. (**C** and **D**) Analysis of recall responses of Id2-deficient (Ly5.2$^+$) and wild-type (Ly5.1$^+$) virus-specific CD8$^+$ T cells. (C) Schematic diagram showing the experimental approach for analyses of memory T cell recall responses. (D) Relative contribution of *Id2*$^{fl/fl}$Lck^{Cre+} CD8$^+$ T cells to the D^{b}NP$_{366}$-specific CD8$^+$ T cell population in spleen, LN, and lung. Data were normalized for the proportion of each genotype represented in the input D^{b}NP$_{366}$$^+$CD8$^+$ T cell population and are expressed as log$_2$ of the ratio of *Id2*$^{fl/fl}$Lck^{Cre+}CD8$^+$D^{b}NP$_{366}$$^+$/wild-type CD8$^+$D^{b}NP$_{366}$$^+$ T cells. Data are pooled from 14 to 18 animals from three independent experiments. Statistically significant differences of the test group to 0 were determined using an unpaired two-tailed Student t test. $^{**}p < 0.01$, $^{***}p < 0.001$.

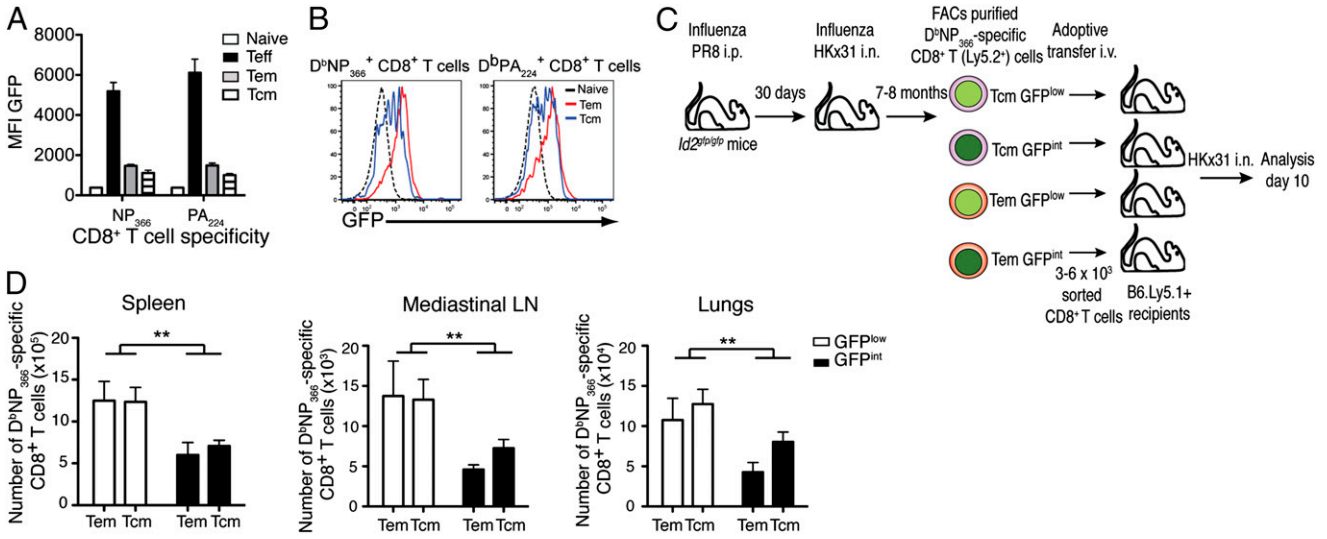

FIGURE 3. Inverse correlation between Id2-GFP expression and memory CD8$^+$ T cell recall capacity. (**A**) *Id2*$^{gfp/gfp}$ mice were infected with HKx31 influenza virus and analyzed 9–10 d (acute) or 12–17 wk (memory) after infection. GFP expression is shown at various stages of virus specific CD8$^+$ T cell differentiation (naive, CD62L$^+$CD44$^-$; effector [acute time point]/effector memory [memory time point], CD62L$^-$CD44$^+$; central memory, CD62L$^+$CD44$^+$). Data are pooled from two independent experiments ($n = 7$) and show the mean Id2-GFP mean fluorescence intensity (MFI) ± SEM. (**B**) HKx31-infected *Id2*$^{gfp/gfp}$ and wild-type mice were analyzed at 17 wk for their expression of Id2-GFP expression in naive (CD44$^-$CD62L$^+$), central memory (Tcm; CD44$^+$ CD62L$^+$), and effector memory (Tem; CD44$^+$CD62L$^-$) in D^{b}NP$_{366}$- and D^{b}PA$_{224}$-specific CD8$^+$ T cells. (**C** and **D**) *Id2*$^{gfp/gfp}$ mice were primed i.p. with PR8 virus, and 4 wk later mice were challenged i.n. with HKx31 influenza virus. Seven to 8 mo after challenge, CD8$^+$ T cells were analyzed. (C) Schematic diagram outlining the isolation and analysis of influenza-specific memory CD8$^+$ T cells expressing different levels of Id2-GFP. (D) Enumeration of the recall capacity of Id2-GFP^{low} and Id2-GFP^{int}D^{b}NP$_{366}$$^+$CD8$^+$ T cells following HKx31 infection as described in (C). D^{b}NP$_{366}$$^+$CD8$^+$ (Ly5.2$^+$, Ly5.1$^-$) isolated from the indicated organs were enumerated by flow cytometry. Data show the means ± SEM of virus-specific CD8$^+$ T cells in the spleen, lungs, and mediastinal LNs pooled from three experiments ($n = 10$). Statistically significant differences were determined using a two-way ANOVA. $^{**}p < 0.01$.

influenza-specific central memory CD8$^+$ T cells had a reduced Id2 expression comparable with naive CD8$^+$ T cells, suggesting that low Id2 expression level is linked to the reported higher recall capacity of central memory T cells (Fig. 3B). To directly test whether Id2 expression determines the recall potential of CD8$^+$ memory T cells, influenza-specific effector memory and central memory T cells from *Id2*$^{gfp/gfp}$ mice were partitioned into cells expressing intermediate (Id2-GFP^{int}) or low (Id2-GFP^{low}) levels of Id2-GFP (Fig. 3C). Following adoptive transfer of each memory T cell subset into congenically marked (Ly5.1$^+$) recipients, analysis of mice infected with HKx31 revealed that regardless of whether transferred D^{b}NP$_{366}$-specific CD8$^+$ T cells were derived from the effector or central memory T cell compartment, the highest proliferative potential was maintained within Id2-GFP^{low} populations (Fig. 3D). These data suggest that Id2 limits the recall potential of memory CD8$^+$ T cells in a dose-dependent manner.

Id2-deficient CD8$^+$ T cells adopt a gene expression signature characteristic of memory precursor cells

To gain insight into how Id2 regulates the lineage choice between effector and memory CD8$^+$ T cells, we compared the gene expression profile of *Id2*^{Lck} and wild-type D^{b}NP$_{366}$-specific CD8$^+$ T cells purified from spleen of *Id2*^{Lck}:Ly5.1 mixed BM chimeras 9 d after HKx31 influenza virus infection by microarray analysis. To ensure that meaningful comparisons could be made between wild-type and *Id2*^{Lck} cells, KLRG1$^+$ cells were excluded during FACS sorting. Two hundred thirty-three differentially expressed (DE) genes were identified (Fold change ≥ 2 and p value ≤ 0.05) (Supplemental Table II). Id2-deficient CD8$^+$ T cells expressed significantly higher levels of key transcriptional regulators important for memory T cell differentiation including *Id3, Tcf7* and *Eomes* (Fig. 4). In contrast, the expression of T-bet and Blimp1, two important regulators of effector T cell differentiation, were markedly reduced in absence of Id2 (Fig. 4B, 4C).

To extend this analysis, we examined how loss of Id2 affected the induction of the effector transcriptional program. Remarkably, the expression of the cytolytic molecules. GzmA and GzmB were significantly reduced in Id2-deficient D^{b}NP$_{366}$-specific CD8$^+$ T cells (Fig. 4A, 4B). Id2-deficient cells also displayed an altered expression of integrins and chemokine receptors such as CD49a, CD103, CX3CR1, and CCR7 likely to impair T cell migration (22–24) (Fig. 4A). This is consistent with our observation that Id2-deficient CD8$^+$ T cell frequency is reduced within nonlymphoid tissues (Fig. 1D). Overall, our data show that Id2-deficient virus-specific CD8$^+$ T cells exhibit an impaired transcriptional program of effector differentiation and consequently fail to appropriately differentiate into short-lived effector CD8$^+$ T cells.

Having established that Id2 was important for memory CD8$^+$ T cells, we speculated that distinct levels of Id2 were deterministic in the transcriptional program of Ag-specific CD8$^+$ T cells. To test this hypothesis, we subjected D^{b}NP$_{366}$-specific effector CD8$^+$ T cells purified according to their differential expression of Id2-GFP (Id2-GFP^{int} and Id2-GFP^{high}) to microarray analysis and compared their gene expression profiles to the 233 DE genes identified by comparing Id2-deficient and wild-type D^{b}NP$_{366}$-specific CD8$^+$ T cells (Supplemental Fig. 2). This analysis revealed that most of the DE genes were strongly dependent on Id2 expression levels. Indeed, 76% of DE genes found to be upregulated in Id2-deficient cells were also upregulated in Id2-GFP^{int} cells compared with Id2-GFP^{high} cells. Similarly, 83% of the DE genes observed to be downregulated in absence of Id2 were downmodulated in Id2-GFP^{int} cells (Supplemental Fig. 2B). Furthermore, expression of *Eomes*, *Id3*, and *Tcf7* mRNA was higher on Id2-GFP^{int} cells compared with Id2-GFP^{high} T cells, whereas GzmB expression was significantly reduced in Id2-GFP^{int} cells T cells (Supplemental Fig. 2B, 2C). However, despite an increased expression of genes involved in memory formation, Id2-GFP^{int} virus-specific CD8$^+$ T cells did not exhibit increased long-

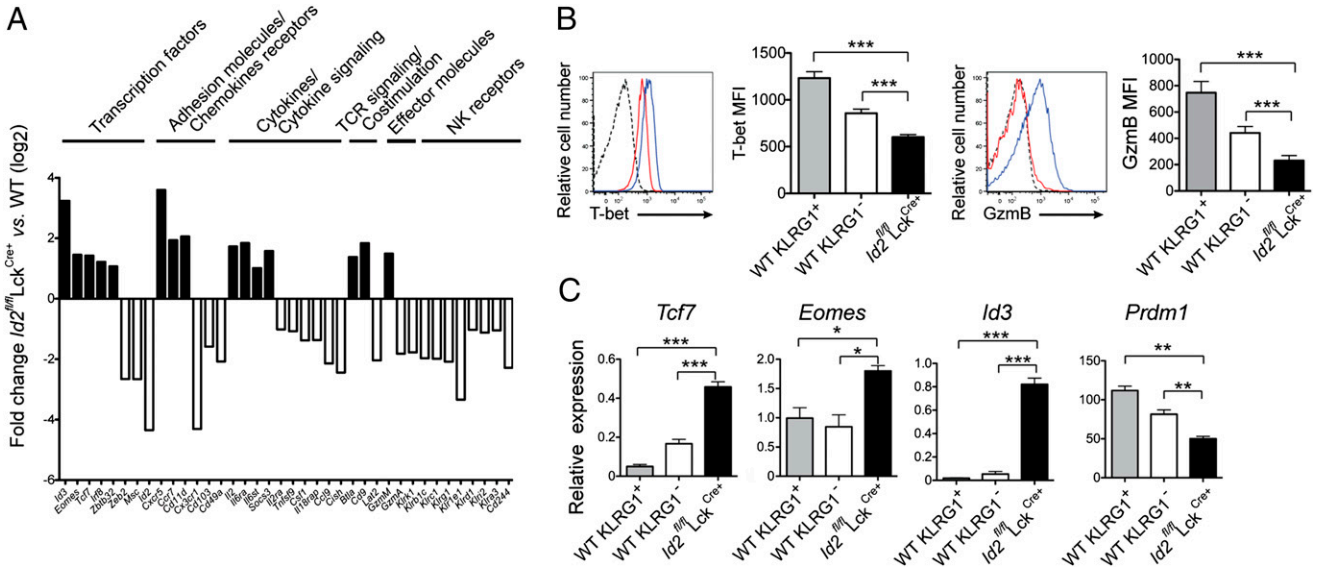

FIGURE 4. Id2-deficient influenza-specific CD8$^+$ T cells express memory signature genes. (**A**) Whole genome analyses of wild-type and *Id2*$^{fl/fl}$Lck^{Cre+} D^{b}NP$_{366}$-specific CD8$^+$ T cells isolated from spleen of PR8-primed/HKx31-infected mice. Graphs show the mean fold difference of 37 (of 233) DE genes between *Id2*$^{fl/fl}$Lck^{Cre+} and wild-type D^{b}NP$_{366}$-specific CD8$^+$ T cells. Genes were selected based on their role in T cell function, migration, and differentiation. Data are pooled from three biologically independent samples. (**B**) Flow cytometric analysis of T-bet and GzmB was compared for naive CD44$^-$ CD8$^+$ T cells (dotted black line) and *Id2*$^{fl/fl}$Lck^{Cre+} (Ly5.2$^+$; solid red line) and wild-type (Ly5.1$^+$; solid blue line) D^{b}NP$_{366}$-specific CD8$^+$ T cells from PR8-primed mixed bone marrow chimeras 9 d after HKx31 infection. Bar graph shows means ± SEM of the mean fluorescence intensity (MFI) of staining for intracellular protein expression within wild-type D^{b}NP$_{366}$$^+$KLRG1$^+$, KLRG1$^-$, or *Id2*$^{fl/fl}$Lck^{Cre+} CD8$^+$ T cells from PR8-primed HKx31 infected mice. Data are pooled from 16 to 20 chimeric mice from three independent experiments. (**C**) Quantitative analysis of mRNA expression by RT-PCR within wild-type D^{b}NP$_{366}$$^+$KLRG1$^+$, KLRG1$^-$, or *Id2*$^{fl/fl}$Lck^{Cre+} CD8$^+$ T cells from PR8-primed HKx31-infected mice (day 9) and naive splenic CD44$^-$CD62L$^+$ CD8$^+$ T cells. Data show the means ± SEM of gene expression relative to that found in naive CD8$^+$ T cells expression from three independent samples. Statistically significant differences were determined using a paired (B) or an unpaired (C) two-tailed Student *t* test. *$p < 0.05$, **$p < 0.01$, ***$p < 0.001$.

term survival compared with Id2-GFP^{high} virus-specific CD8$^+$ T cells (Supplemental Fig. 2D, 2E). This indicated that the survival of memory cells is not dictated by the level of Id2 expression, consistent with our previous results (Fig. 2B).

Overall, our data demonstrate that the transcriptional program of CD8$^+$ T cell differentiation is exquisitely sensitive to the concentration of Id2.

Id2 controls effector differentiation by inhibiting E2A

Id2 is a key negative regulator of the E protein transcription factor family but it is less clear which specific E protein Id2 might act on during T cell differentiation. We hypothesized that Id2 controls CD8$^+$ T cell differentiation by limiting the transcriptional activity of E2A. To investigate this question, we transduced wild-type and *Id2*^{Lck} OT-I T cells with retroviruses encoding either a shRNA against *Tcfe2a* (encoding E2A) or a control hairpin and then analyzed the expression of key target genes identified as DE in our previous microarray analysis. The *Tcfe2a* shRNA induced an 80% reduction of *Tcfe2a* expression, and this reduction was not compensated by an increased of the other E protein family members *Tcf12* (encoding HEB) and *Tcf4* (encoding E2.2) expression (Fig. 5A). Remarkably, silencing of *Tcfe2a* in Id2^{Lck} OT-I T cells and, to a lesser extent, in wild-type OT-I T cells resulted in a decrease in the expression of several genes important for the development and/or the maintenance of memory T cells, such as *Tcf7*, *Id3*, and *Socs3* (2, 3, 9, 25) (Fig. 5A). In contrast, Id2^{Lck} OT-I T cells transduced with the *Tcf2e2a* shRNA exhibited an increased expression of genes encoding the effector molecules GzmB and GzmK compared with cells transduced with the control shRNA retrovirus (Fig. 5A). Of note, the expression of *Tbx21* or *Prdm1* was not affected by *Tcfe2a* knockdown in vitro, suggesting that they are not direct targets of E2A.

To confirm the involvement of E2A, we then wanted to determine the proportion of genes having E2A occupancy at promoter/enhancer distance among the list of 233 DE genes in the absence of Id2. We took advantage of *Tcfe2a*$^{Bio/Bio}$ mice (I. Bilic and M. Busslinger, unpublished observations), which express an E2A-Bio protein containing a C-terminal biotin acceptor sequence that is efficiently biotinylated in vivo by coexpression of the *Escherichia coli* biotin ligase BirA from the *Rosa26*^{BirA} allele. We then determined the genome-wide pattern of E2A binding in total thymocytes from *Tcfe2a*$^{Bio/Bio}$ mice, in which Id2 expression is low (27) and hence allows high E2A binding to its target genes. Using a stringent *p* value of $<10^{-10}$ for peak calling, we detected 4337 E2A-binding regions, which defined 2541 E2A target genes in total thymocytes. We next used these E2A target genes to cross-reference our microarray data comparing Id2-deficient and wild-type virus-specific CD8$^+$ T cells. Strikingly, the results from this analysis showed that among our list of genes found to be upregulated in absence of Id2, the proportion of those with an E2A-binding site is significantly higher than among all genes of the genome, consistent with the transactivating function of E2A (Fig. 5B). In contrast, there is no significant difference of enrichment of genes with E2A occupancy among the genes found to be downregulated in absence of Id2 compared with the whole genome, suggesting that they are not directly regulated by E2A (Fig. 5B). Consistent with the *Tcfe2a* silencing data (Fig. 5A), our Bio-ChIP sequencing analysis identified several E2A-binding sites at the loci of key genes involved in memory T cell differentiation or function such as *Tcf7*, *Id3*, *Socs3*, or *Ccr7*, whereas no binding sites were detected at the loci of genes associated with an effector phenotype such as *Tbx21*, *Gzmk*, and *Gzmb* (F. Masson and G.T. Belz, unpublished observations). Overall, our results suggest that Id2 restrains memory T cell development by inhibiting E2A transcriptional activity.

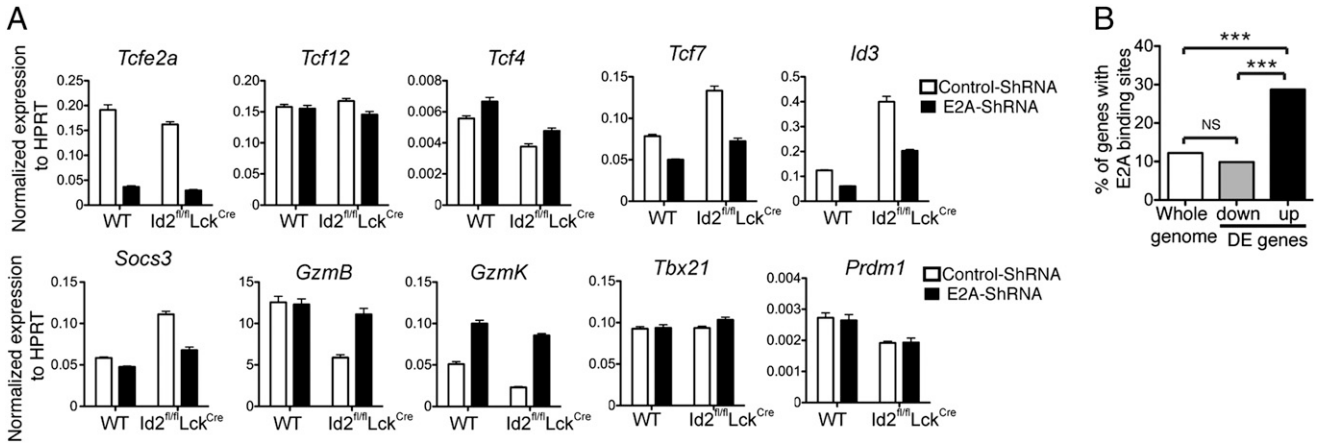

FIGURE 5. Id2 controls effector and memory CD8$^+$ T cell differentiation by inhibiting E2A transcriptional activity. (**A**) Wild-type and *Id2$^{fl/fl}$*Lck^{Cre+} OT-I cells were transduced with shRNA-*tcfe2a*-GFP and shRNA-control-GFP retroviruses. GFP$^+$ cells (95% positive) were subjected to quantitative RT-PCR for the indicated genes. Graphs show the means ± SEM of the experimental triplicates of the expression relative to *Hprt* and are representative of two independent experiments. (**B**) Bio-ChIP sequencing data of total thymocytes from *Tcfe2a*$^{Bio/Bio}$ *Rosa26*$^{BirA/BirA}$ mice. Bar graph shows the proportion of genes with E2A-binding sites in the whole genome or among the 233 DE (upregulated or downregulated) genes in Id2-deficient virus-specific CD8$^+$ T cells. Statistically significant differences were determined using a Fisher exact test. ***$p < 0.001$.

E2A regulates Tcf7 *expression in peripheral CD8$^+$ T cells*

Tcf7, a critical regulator of memory CD8$^+$ T cell differentiation, persistence, and recall potential (9), was significantly upregulated in Id2-deficient CD8$^+$ T cells (Fig. 4C) and correlated with the dose of Id2 (Fig. 4D). *Tcf7* expression was also downregulated in Id2-deficient T cells in which E2A was silenced (Fig. 5A). Our Bio-ChIP sequencing analysis in total thymocytes identified several E2A-binding sites at the *Tcf7* locus (Fig. 6A). However, because Id2 is not expressed in double-positive thymocytes (27) whereas it is expressed at low level in naive CD8$^+$ T cells (Fig. 1B) and at a high level in effector CD8$^+$ T cells (Fig 1B), the binding of E2A to the Tcf7 locus is expected to be inversely correlated to the level of Id2 expression in these different T cell subsets. Therefore, we then investigated whether *Tcf7* was also a direct target of E2A in peripheral CD8$^+$ T cells. Using conventional ChIP-quantitative PCR analysis, we tested whether E2A could bind to these sequences also in naive and in vitro–activated CD8$^+$ T cells. In naive CD8$^+$ T cells, E2A no longer bound to site 2 and interacted weakly with sites 1, 3, and 5 in contrast to thymocytes (Fig. 6B). However, E2A efficiently bound to site 4 (located 33 kb upstream of the *Tcf7* transcription starting start), suggesting that E2A activates the *Tcf7* gene through this upstream enhancer in naive CD8$^+$ T cells. Critically, the interaction of E2A with site 4 and the weaker binding sites was lost following activation and concurrent induction of Id2 expression (Fig. 6B), suggesting that E2A directly regulated *Tcf7* expression in a manner that was inhibited in the presence of Id2.

Id2-dependent control of T-bet expression is required for the differentiation of short-lived effector cells

T-bet is a key transcriptional regulator of effector differentiation that is downregulated in the absence of Id2 (Fig. 4B). Because T-bet promotes short-lived effector cell differentiation in a dose-dependent manner (10), we speculated that the reduction of T-bet expression observed in *Id2^{Lck}* T cells might be responsible for the observed defect in short-lived effector CD8$^+$ T cell formation. In line with this hypothesis, analysis of mixed bone marrow chimeras created using wild-type (Ly5.1$^+$) and *Tbx21$^{+/-}$* (Ly5.2$^+$) heterozygous bone marrow revealed that a 2-fold reduction of T-bet (Fig. 7A), similar to that observed in *Id2^{Lck}* T cells (Fig. 4B), was sufficient to impair the generation of short-lived effector T cells after influenza infection (Fig. 7B).

To test whether downregulation of T-bet expression in Id2-deficient CD8$^+$ T cells was directly responsible for the loss of effector CD8$^+$ T cells, we transduced *Id2^{Lck}* OT-I CD8$^+$ T cells with retroviruses encoding T-bet or Id2 or with a control retrovirus. In vitro–activated transduced *Id2^{Lck}* and wild-type OT-I T cells were adoptively transferred into Ly5.1$^+$ recipient mice. Mice were infected with Lm-OVA 24 h later. After 8 d, the formation of effector CD8$^+$ T cells from transduced OT-I cells was

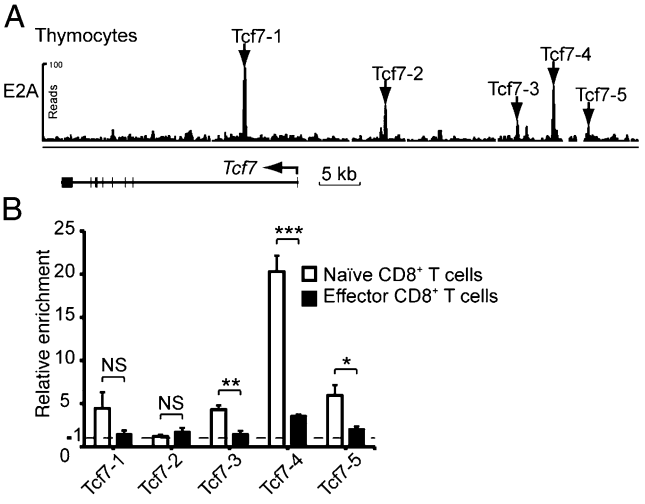

FIGURE 6. E2A binding to the *Tcf7* locus of peripheral CD8$^+$ T cells is lost following effector differentiation in vitro. (**A**) Identification of E2A-binding regions at the *Tcf7* locus by ChIP sequencing of total thymocytes. Arrows indicate the sites tested for E2A binding in (**B**). (B) ChIP analysis of E2A binding in naive and in vitro activated effector CD8$^+$ T cells. Input and precipitated DNA were quantified by real-time PCR with primer pairs amplifying the indicated E2A-binding regions of the *Tcf7* locus [shown in (A)] and a geneless control region of mouse chromosome 1 (Supplemental Table II). The relative enrichment of E2A binding was determined by dividing the percentage of precipitated DNA at the E2A-binding site (ChIP/input) by the percentage of precipitated DNA at the geneless control region of mouse chromosome 1 (ChIP/input). The relative enrichment of E2A binding is shown as means ± SEM of three independent ChIP experiments. No enrichment is indicated by a dashed line. Statistically significant differences were determined using an unpaired two-tailed Student *t* test. *$p < 0.05$, **$p < 0.01$, ***$p < 0.001$.

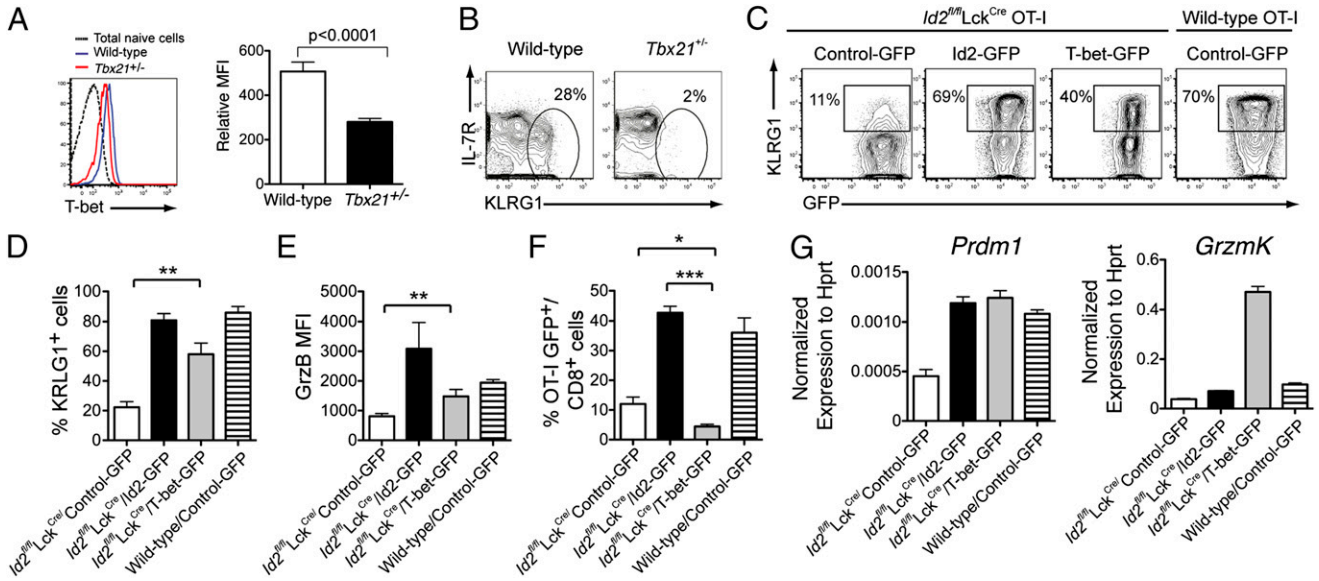

FIGURE 7. Enforced expression of *Tbx21* rescues differentiation of Id2-deficient short-lived effector cells. (**A** and **B**) PR8-primed mixed bone marrow chimeras reconstituted with a mix of *Tbx21* heterozygote (+/−, Ly5.2) and wild-type (+/+, Ly5.1) bone marrow cells were analyzed 9 d after HKx31 i.n. infection. (A) Histogram (*left panel*) and mean fluorescence intensitiy (MFI) (*right panel*) of expression of T-bet in naive ($CD44^-$, black line) or activated D^bNP-specific $CD8^+$ T cells gated on wild-type ($Ly5.1^+$, blue line) or $Tbx21^{+/-}$ ($Ly5.2^+$, red line) $CD8^+$ T cell compartments from mixed bone marrow chimeras. Data show the means ± SEM ($n = 11$ animals pooled from three independent experiments). (B) Representative contour plots showing IL-7R and KLRG1 expression in D^bNP_{366}-specific $CD8^+$ T cells. Statistically significant differences were determined using a paired two-tailed Student *t* test. (**C**–**F**) Wild-type ($Ly5.1^+$) and $Id2^{fl/fl}Lck^{Cre+}$ ($Ly5.2^+$) OT-I cells were transduced with control-GFP, Id2-GFP, or T-bet-GFP retroviruses. One week after activation, GFP^+ cells were transferred into recipient mice that were then infected with Lm-OVA. Eight days after infection, mice were sacrificed and OT-I T cell response was analyzed in the spleen. (C) Flow cytometric analysis of KLRG1 and GFP expression on transduced $GFP^+Id2^{fl/fl}Lck^{Cre+}$ ($Ly5.2^+$) OT-I T cells or wild-type ($Ly5.1^+$) OT-I T cells 8 d after infection with Lm-OVA. Data are pooled from five to six animals for each condition from two independent experiments. (D) Analysis of the frequency of $KLRG1^+$ cells within the $GFP^+Id2^{fl/fl}Lck^{Cre+}$ or wild-type OT-I T cells that had been transduced with the indicated vectors. Data show the mean percentage ± SEM for spleen with at least five mice for each group pooled from two independent experiments. (E) Bar graph shows mean ± SEM of the MFI of staining for intracellular GzmB expression within $GFP^+Id2^{fl/fl}Lck^{Cre+}$ or wild-type OT-I T cells that had been transduced with the indicated vectors. Data are pooled from five to six mice from two independent experiments. (F) Bar graph shows the frequency of OT-I $Ly5.2^+CD8^+$ T cells transduced with the indicated vectors among the total $CD8^+$ T cell population from the spleen 8 d after Lm-OVA infection and is representative of two experiments with three mice per group in each experiments. Statistically significant differences were determined using an unpaired two-tailed Student *t* test. $^*p < 0.05$, $^{**}p < 0.01$, $^{***}p < 0.001$. (**G**) Quantitative analysis of mRNA expression by RT-PCR within GFP^+ wild-type or $Id2^{fl/fl}Lck^{Cre+}$ OT-I T cells that had been transduced with the indicated vectors. Bar graph represents the means ± SEM of the experimental triplicates of the expression relative to *Hprt*. Data are representative of two independent experiments.

evaluated (Fig. 7C). Re-expression of Id2 into Id2-deficient OT-I cells rescued the development of $KLRG1^+$ effector cells. Transduction of Id2-deficient OT-I T cells with the T-bet retrovirus resulted in the rescue of T-bet expression to a level similar to Id2-deficient $CD8^+$ T cells transduced with the Id2 retrovirus (F. Masson and G.T. Belz, unpublished observations). Strikingly, Id2-deficient OT-I cells overexpressing T-bet were also able to form $KLRG1^+$ effector T cells in similar frequency (Fig. 7C, 7D). Additionally, T-bet overexpression partly rescued GzmB expression in vivo and *Prdm1* and *GzmK* mRNA expression after in vitro culture in the presence of IL-2 (Fig. 7E, 7G). T-bet overexpressing OT-I cells, however, did not expand as well as OT-I cells transduced with Id2 or the control vector (Fig. 7F), consistent with the observation that T-bet overexpression increase activation-induced cell death in $CD8^+$ T cells (28). Collectively, our data indicate that Id2 is required to induce sufficient *Tbx21* expression to generate short-lived effector $CD8^+$ T cells.

Discussion

Id2 is a key regulator of $CD8^+$ T cell–mediated immunity, but there is a limited understanding of the molecular mechanisms by which Id2 exerts its effects influencing effector and memory T cell fate decisions. Early studies suggested that the main action of Id2 is to ensure the survival of effector $CD8^+$ T cells following activation (1). In contrast, our study shows the absence of a major defect in the overall survival of virus-specific $CD8^+$ T cell during influenza infection and this has allowed us to dissociate the differentiation defect from the survival defect reported in the former studies. Our data support an alternate model in which Id2 can act as a rheostat to directly regulate the differentiation of naive $CD8^+$ T cells into effector or memory T cells. We demonstrated that Id2 limits memory $CD8^+$ T cell formation and recall potential in a dose-dependent manner by inhibiting E2A transcriptional activity. In particular, Id2 inhibits E2A-mediated transactivation of *Tcf7*. Finally, we showed that Id2 is required for the optimal induction of T-bet and thereby for the differentiation of $KLRG1^+$ short-lived effector cells.

Id2 deficiency resulted in a profound alteration of the transcriptional program that drives the differentiation of virus-specific $CD8^+$ T cells. Id2-deficient cells exhibit an increased expression in multiple genes involved in memory T cell differentiation and function (*Tcf7*, *Id3*, *Socs3*, *Eomes*, *Il2*, *Ccr7*) paralleled by a concurrent decrease in the expression of genes associated with an effector phenotype (*Tbx21*, *Prdm1*, *Il2rα*, *Grzma*, *Gzmb*, *Gzmk*, *Cd103*, *Cx3cr1*, *Cd49a*). Remarkably, the comparison of our microarray data analysis with E2A CHIP sequencing data revealed that there was a significant enrichment for genes with E2A-binding sites among the genes upregulated in absence of Id2 compared with the DE genes that were downregulated. This suggests that Id2 represses the memory program of $CD8^+$ T cell

differentiation by inhibiting the E2A-mediated transactivation of several key genes involved in the process of memory differentiation such as *Tcf7*.

Tcf7 is a key mediator of the Wnt/β-catenin signaling pathway essential for the generation and the persistence of memory T cells through its control of *Eomes* expression, as well as for the recall potential of memory $CD8^+$ T cells (9). *Tcf7* is highly expressed in naive $CD8^+$ T cells and is downregulated in effector $CD8^+$ T cells. We showed that both *Tcf7* and *Eomes* were expressed at higher levels in Id2-deficient effector $CD8^+$ T cells compared with wild-type effector T cells. Using E2A ChIP analyses, we discovered that E2A directly binds to the *Tcf7* locus and this binding is lost following activation concurrent with the induction of Id2. Finally, silencing of *Tcf2ea* in Id2-deficient $CD8^+$ T cells resulted in the downregulation of *Tcf7* expression. Taken together, these data suggest that a major pathway by which Id2 restrains the formation of memory precursor cells is by inhibiting the E2A-dependent activation of *Tcf7* in effector $CD8^+$ T cells.

Recently it has been proposed that the repression of *Id3* by Blimp1 promoted the development of effector T cells at the expense of memory cell differentiation (2). In our studies, in the absence of Id2, Id3 was strongly upregulated (Figs. 2D, 5A) whereas silencing of *Tcfe2a* in Id2-deficient $CD8^+$ T cells reversed this upregulation of Id3 in Id2-deficient $CD8^+$ T cells in vitro without affecting Blimp1 expression (Fig. 5A). From our E2A ChIP sequencing data, we identified several binding sites at the *Id3* locus (F. Masson and G.T. Belz, unpublished observations), confirming that *Id3* is a direct target of E2A. It has also been reported that Id3-deficient $CD8^+$ T cells did not show any reduction in memory precursor cell frequency (or increase in the frequency of short-lived effector T cells) (2). Thus, repression of *Id3* does not appear to influence the lineage choice decision between effector and memory cells at the acute time point of an infection, although it does affect the maintenance of memory cells in the long term. From our studies, we propose that Id3 expression is directly influenced by Id2 expression dynamics, which in turn regulates the E2A-dependent transcriptional activation of the *Id3* locus. Thus, Id2 rather than Id3 expression level delineates the effector and memory phenotype during the acute phase of an infection.

Id2 and Id3 are both known to interact with the same basic helix-loop-helix partners (11, 29), but it is not clear whether they bind different E proteins with a similar affinity. Indeed, Id2 and Id3 have clearly different functions in effector and memory cells. This is exemplified by the loss of long-term memory cells in absence of Id3 as opposed to the loss of short-lived effector cells observed in the absence of Id2 (1, 3). We have shown in this study that reduction or loss of Id2 expression in endogenous virus-specific memory $CD8^+$ T cells leads to enhanced recall responses. In contrast, Id3 overexpression improved the magnitude of the recall response of memory $CD8^+$ T cells (2). In this latter setting, it is not clear whether this represents the physiological action of Id3. Given the contrasting roles of Id3 and Id2 in T cell differentiation, it will be crucial to determine with which E protein partners each Id protein interacts when expressed at physiological levels. This partner could be E2A or another member of the E protein family (HEB and E2-2). Indeed, HEB has been recently reported to collaborate with E2A in the generation of memory cells (30). However, it may also be another protein unrelated to the E protein family. Indeed, even though E proteins have been described as the main heterodimerizing partners of Id proteins, other proteins such as the myogenic factors PU.1 and Rb have been described to interact with Id2 (31–33).

Our microarray data analysis has shown that many genes involved in effector differentiation and/or functions were downregulated in absence of Id2. In particular, the expression of T-bet, a key transcriptional regulator of effector T cell differentiation, was also affected. Our results suggest that T-bet expression is indirectly regulated by E2A because no E protein binding sites were detected at its locus using in silico bioinformatical analysis, or ChIP sequencing in whole thymocytes (F. Masson and G.T. Belz, unpublished observations), or in the A12 T cell line (34). It is therefore likely that the decrease in the expression of this key transcriptional regulator is a consequence of the altered differentiation of Id2-deficient $CD8^+$ T cells toward the memory phenotype. Surprisingly, E2A silencing did not affect *Tbx21* expression in vitro (Fig. 5A), suggesting that either the level of E2A silencing was insufficient to induce a significant change of T-bet expression or that other E protein family members HEB and E2-2 may compensate for the loss of E2A in the regulation of T-bet expression. Further analyses showed that decreased expression of T-bet was responsible for the loss of $KLRG1^+$ cells in Id2-deficient $CD8^+$ T cells. In support of this finding, haploinsufficiency of *Tbx21* (a decrease in T-bet expression comparable to the downregulation induced by Id2 ablation) was sufficient to block short-lived $CD8^+$ effector T cell differentiation (Fig. 7B) (10), and enforced expression of T-bet in Id2-deficient $CD8^+$ T cells rescued short-lived effector T cell differentiation (Fig. 7C, 7D).

In conclusion, our study has identified Id2 as a critical dosage-dependent regulator of E protein transcriptional activity, in particular E2A, which determines whether a naive $CD8^+$ T cell will commit to effector or memory differentiation. We propose a model in which Id2 promotes effector differentiation by restraining the E2A-mediated transactivation of several key genes essential for memory T cell development and function.

Acknowledgments

We thank Annie Xin, Wei Shi, Malou Zuidscherwoude, Philippe Bouillet, Marc Pellegrini, Lynn Corcoran, Ross Dickins, Manabu Sugai, Simon Preston, and Mary Camilleri for provision of reagents, advice, and technical assistance, and Markus Jaritz for bioinformatic analysis.

Disclosures

The authors have no financial conflicts of interest.

References

1. Cannarile, M. A., N. A. Lind, R. Rivera, A. D. Sheridan, K. A. Camfield, B. B. Wu, K. P. Cheung, Z. Ding, and A. W. Goldrath. 2006. Transcriptional regulator Id2 mediates $CD8^+$ T cell immunity. *Nat. Immunol.* 7: 1317–1325.
2. Ji, Y., Z. Pos, M. Rao, C. A. Klebanoff, Z. Yu, M. Sukumar, R. N. Reger, D. C. Palmer, Z. A. Borman, P. Muranski, et al. 2011. Repression of the DNA-binding inhibitor Id3 by Blimp-1 limits the formation of memory $CD8^+$ T cells. *Nat. Immunol.* 12: 1230–1237.
3. Yang, C. Y., J. A. Best, J. Knell, E. Yang, A. D. Sheridan, A. K. Jesionek, H. S. Li, R. R. Rivera, K. C. Lind, L. M. D'Cruz, et al. 2011. The transcriptional regulators Id2 and Id3 control the formation of distinct memory $CD8^+$ T cell subsets. *Nat. Immunol.* 12: 1221–1229.
4. Intlekofer, A. M., N. Takemoto, E. J. Wherry, S. A. Longworth, J. T. Northrup, V. R. Palanivel, A. C. Mullen, C. R. Gasink, S. M. Kaech, J. D. Miller, et al. 2005. Effector and memory $CD8^+$ T cell fate coupled by T-bet and eomesodermin. *Nat. Immunol.* 6: 1236–1244.
5. Kallies, A., A. Xin, G. T. Belz, and S. L. Nutt. 2009. Blimp-1 transcription factor is required for the differentiation of effector $CD8^+$ T cells and memory responses. *Immunity* 31: 283–295.
6. Shin, H., S. D. Blackburn, A. M. Intlekofer, C. Kao, J. M. Angelosanto, S. L. Reiner, and E. J. Wherry. 2009. A role for the transcriptional repressor Blimp-1 in $CD8^+$ T cell exhaustion during chronic viral infection. *Immunity* 31: 309–320.
7. Rutishauser, R. L., G. A. Martins, S. Kalachikov, A. Chandele, I. A. Parish, E. Meffre, J. Jacob, K. Calame, and S. M. Kaech. 2009. Transcriptional repressor Blimp-1 promotes $CD8^+$ T cell terminal differentiation and represses the acquisition of central memory T cell properties. *Immunity* 31: 296–308.
8. Ichii, H., A. Sakamoto, M. Hatano, S. Okada, H. Toyama, S. Taki, M. Arima, Y. Kuroda, and T. Tokuhisa. 2002. Role for Bcl-6 in the generation and maintenance of memory $CD8^+$ T cells. *Nat. Immunol.* 3: 558–563.

9. Zhou, X., S. Yu, D. M. Zhao, J. T. Harty, V. P. Badovinac, and H. H. Xue. 2010. Differentiation and persistence of memory $CD8^+$ T cells depend on T cell factor 1. *Immunity* 33: 229–240.
10. Joshi, N. S., W. Cui, A. Chandele, H. K. Lee, D. R. Urso, J. Hagman, L. Gapin, and S. M. Kaech. 2007. Inflammation directs memory precursor and short-lived effector $CD8^+$ T cell fates via the graded expression of T-bet transcription factor. *Immunity* 27: 281–295.
11. Engel, I., and C. Murre. 2001. The function of E- and Id proteins in lymphocyte development. *Nat. Rev. Immunol.* 1: 193–199.
12. Jackson, J. T., Y. Hu, R. Liu, F. Masson, A. D'Amico, S. Carotta, A. Xin, M. J. Camilleri, A. M. Mount, A. Kallies, et al. 2011. Id2 expression delineates differential checkpoints in the genetic program of $CD8\alpha^+$ and $CD103^+$ dendritic cell lineages. *EMBO J.* 30: 2690–2704.
13. Rankin, L., and G. T. Belz. 2011. Diverse roles of inhibitor of differentiation 2 in adaptive immunity. *Clin. Dev. Immunol.* 2011: 281569.
14. Finotto, S., M. F. Neurath, J. N. Glickman, S. Qin, H. A. Lehr, F. H. Green, K. Ackerman, K. Haley, P. R. Galle, S. J. Szabo, et al. 2002. Development of spontaneous airway changes consistent with human asthma in mice lacking T-bet. *Science* 295: 336–338.
15. Hogquist, K. A., S. C. Jameson, W. R. Heath, J. L. Howard, M. J. Bevan, and F. R. Carbone. 1994. T cell receptor antagonist peptides induce positive selection. *Cell* 76: 17–27.
16. Farley, F. W., P. Soriano, L. S. Steffen, and S. M. Dymecki. 2000. Widespread recombinase expression using FLPeR (flipper) mice. *Genesis* 28: 106–110.
17. Hennet, T., F. K. Hagen, L. A. Tabak, and J. D. Marth. 1995. T-cell-specific deletion of a polypeptide *N*-acetylgalactosaminyl-transferase gene by site-directed recombination. *Proc. Natl. Acad. Sci. USA* 92: 12070–12074.
18. Driegen, S., R. Ferreira, A. van Zon, J. Strouboulis, M. Jaegle, F. Grosveld, S. Philipsen, and D. Meijer. 2005. A generic tool for biotinylation of tagged proteins in transgenic mice. *Transgenic Res.* 14: 477–482.
19. Seillet, C., J. T. Jackson, K. A. Markey, H. J. Brady, G. R. Hill, K. P. Macdonald, S. L. Nutt, and G. T. Belz. 2013. $CD8\alpha^+$ DCs can be induced in the absence of transcription factors Id2, Nfil3, and Batf3. *Blood.* 121: 1574–1583.
20. Belz, G. T., W. Xie, J. D. Altman, and P. C. Doherty. 2000. A previously unrecognized H-$2D^b$-restricted peptide prominent in the primary influenza A virus-specific $CD8^+$ T-cell response is much less apparent following secondary challenge. *J. Virol.* 74: 3486–3493.
21. Belz, G. T., N. S. Wilson, C. M. Smith, A. M. Mount, F. R. Carbone, and W. R. Heath. 2006. Bone marrow-derived cells expand memory $CD8^+$ T cells in response to viral infections of the lung and skin. *Eur. J. Immunol.* 36: 327–335.
22. Ebert, A., S. McManus, H. Tagoh, J. Medvedovic, G. Salvagiotto, M. Novatchkova, I. Tamir, A. Sommer, M. Jaritz, and M. Busslinger. 2011. The distal V_H gene cluster of the *Igh* locus contains distinct regulatory elements with Pax5 transcription factor-dependent activity in pro-B cells. *Immunity* 34: 175–187.
23. Chapman, T. J., and D. J. Topham. 2010. Identification of a unique population of tissue-memory $CD4^+$ T cells in the airways after influenza infection that is dependent on the integrin VLA-1. *J. Immunol.* 184: 3841–3849.
24. Masson, F., T. Calzascia, W. Di Berardino-Besson, N. de Tribolet, P. Y. Dietrich, and P. R. Walker. 2007. Brain microenvironment promotes the final functional maturation of tumor-specific effector $CD8^+$ T cells. *J. Immunol.* 179: 845–853.
25. Mionnet, C., V. Buatois, A. Kanda, V. Milcent, S. Fleury, D. Lair, M. Langelot, Y. Lacoeuille, E. Hessel, R. Coffman, et al. 2010. CX3CR1 is required for airway inflammation by promoting T helper cell survival and maintenance in inflamed lung. *Nat. Med.* 16: 1305–1312.
26. Cui, W., Y. Liu, J. S. Weinstein, J. Craft, and S. M. Kaech. 2011. An interleukin-21-interleukin-10-STAT3 pathway is critical for functional maturation of memory $CD8^+$ T cells. *Immunity* 35: 792–805.
27. Jones-Mason, M. E., X. Zhao, D. Kappes, A. Lasorella, A. Iavarone, and Y. Zhuang. 2012. E protein transcription factors are required for the development of $CD4^+$ lineage T cells. *Immunity* 36: 348–361.
28. Yeo, C. J., and D. T. Fearon. 2011. T-bet-mediated differentiation of the activated $CD8^+$ T cell. *Eur. J. Immunol.* 41: 60–66.
29. Kee, B. L. 2009. E and ID proteins branch out. *Nat. Rev. Immunol.* 9: 175–184.
30. D'Cruz, L. M., K. C. Lind, B. B. Wu, J. K. Fujimoto, and A. W. Goldrath. 2012. Loss of E protein transcription factors E2A and HEB delays memory-precursor formation during the $CD8^+$ T-cell immune response. *Eur. J. Immunol.* 42: 2031–2041.
31. Langlands, K., X. Yin, G. Anand, and E. V. Prochownik. 1997. Differential interactions of Id proteins with basic-helix-loop-helix transcription factors. *J. Biol. Chem.* 272: 19785–19793.
32. Lasorella, A., M. Noseda, M. Beyna, Y. Yokota, and A. Iavarone. 2000. Id2 is a retinoblastoma protein target and mediates signalling by Myc oncoproteins. *Nature* 407: 592–598.
33. Ji, M., H. Li, H. C. Suh, K. D. Klarmann, Y. Yokota, and J. R. Keller. 2008. Id2 intrinsically regulates lymphoid and erythroid development via interaction with different target proteins. *Blood* 112: 1068–1077.
34. Lin, Y. C., S. Jhunjhunwala, C. Benner, S. Heinz, E. Welinder, R. Mansson, M. Sigvardsson, J. Hagman, C. A. Espinoza, J. Dutkowski, et al. 2010. A global network of transcription factors, involving E2A, EBF1 and Foxo1, that orchestrates B cell fate. *Nat. Immunol.* 11: 635–643.